INSIGHTS INTO THE FORMATION OF CENTRAL PIT CRATERS. N. G. Barlow[1] and L. L. Tornabene[2], [1]Dept. Physics and Astronomy, Northern Arizona University, Flagstaff, AZ 86011-6010 Nadine.Barlow@nau.edu. [2]CPSX and Dept. Earth Sciences, Western University, London, ON N6A 5B ltornabe@uwo.ca.

Introduction: Central pit craters have been reported on bodies with ice-rich crusts (Ganymede, Callisto, Ceres, and Pluto), intermediate rock/ice crusts (Mars), and volatile-poor crusts (Moon, Mercury). They are distinguished by the presence of a central depression either directly on the crater floor (elevation of pit floor below elevation of crater floor; "floor pit") or atop a central peak (elevation of pit floor above elevation of crater floor; "summit pit") [1] (Fig. 1). The depression is generally approximately circular to elliptical in shape and is distinct form the irregular pits inside craters associated with endogenic processes [e.g., 2]. Floor pits can be further subdivided into whether the pit has a raised rim extending entirely or part-way around the pit edge, or if no raised rim is seen [3].

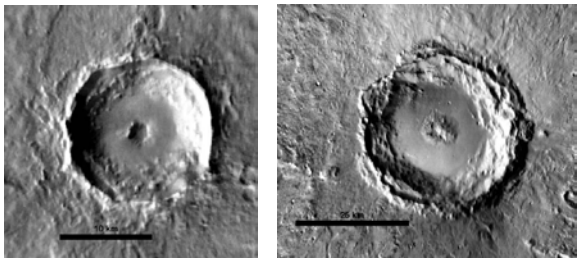

Figure 1: (Left) 16.3-km-D Esira crater (8.95°N 313.40°E) contains a 2.5-km-D partially rimmed floor pit. (Right) This unnamed 33.8-km-D crater (35.83°N 319.21°E) contains a 3.4-km-D summit pit. (THEMIS mosaics)

Current Study: Numerous models have been proposed regarding the formation of central pits within craters, many of which require the presence of target volatiles [4-11]. The current study is the first comparison study of central pit craters across the solar system and is conducting detailed geologic mapping of selected fresh central pit craters on Mars to help constrain the formation of these features. The following bodies and datasets are used for the database compilation: Mercury MESSENGER MDIS 250 m/pixel global mosaic; Moon LRO WAC 100 m/pixel global mosaic; Mars THEMIS daytime IR 100 m/pixel global mosaic; Ganymede and Callisto Voyager and Galileo global mosaics (60 km/pixel to 400 m/pixel resolutions); and Dione, Rhea, and Tethys Voyager and Cassini global mosaics (250-400 m/pixel). Central pits on Ceres and Pluto will be added to the study soon. These global surveys include information on the latitude, longitude, and diameter (D_c) of the parent crater, geologic unit, crater preservational state, geologic unit, type of pit (floor or summit), pit diameter (D_p), pit-to-crater diameter ratio (D_p/D_c), peak basal diameter for summit pit craters (D_{pk}), and peak-to-crater diameter ratio for summit pits (D_{pk}/D_c). Detailed geologic mapping of selected Martian central pit craters is being conducted using ArcGIS with the following datasets: MOLA (~100 m/pixel resolution), THEMIS daytime and nighttime IR (100 m/pixel), THEMIS visible (18 m/pixel), CRISM (15-19 m/pixel in targeted mode), CTX (6 m/pixel), and HiRISE (up to 30 cm/pixel).

General Trends: General trends from our preliminary results of the comparison study of central pit craters on Mercury, the Moon Mars, Ganymede, and the Saturnian satellites include:

- No correlation of central pit craters with specific geologic units has been observed on any body.
- Floor pits tend to be larger relative to their parent crater than summit pits.
- Central pit craters are rarer on bodies with volatile-poor crusts and on bodies with low surface gravity.
- Floor pits become more prevalent as the concentration of crustal volatiles increases.
- D_p/D_c is consistently higher for central pits on bodies with volatile-rich crusts (Ganymede, Tethys, Dione, and Rhea) and is lower on bodies with volatile-poor crusts (Moon, Mercury). Mars is an intermediate case.
- D_p/D_c tends to increase as gravity increases from the Moon to Mercury to Mars. A similar trend is not seen among Tethys, Dione, Rhea, and Ganymede, however.

Mapping of Martian Central Pit Craters: We have selected different types of central pit craters which display characteristics of freshness in order to determine primary morphologic characteristics of central pits. We have completed mapping of the 16.3-km-D partially rimmed floor pit crater Esira (Fig. 1-2). The pit rim is uplifted above the crater floor on the western half of the pit, but thermal inertia analysis suggests uplifted bedrock just below the crater floor surface on the unexposed eastern side as well. Uplift of layered bedrock and megabreccias have been previously reported for other central pit and cental peak craters [e.g., 12]. We also find that pitted material on Esira's floor flows into the central pit. Pitted material has been argued to form as impact melt interacts with near-surface volatiles [13-14], with the diameters of the pits within the pitted material being related to the thickness

of the impact melt deposit [13]. In Esira, the pitted material pits have larger diameters within the central pit than those on the crater floor, which is consistent with the impact melt having greater thickness as it ponded within the confines of the central floor pit.

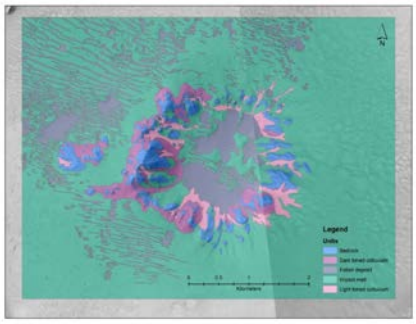

Figure 2: Geologic map of the central pit of Esira crater.

We are close to finishing the mapping of an unnamed 33.8-km-D summit pit crater (Fig. 1). Although the pit contains large amounts of mass wasting and aeolian debris, we have identified outcrops of pitted material in the southern part of the pit (Fig. 3). The presence of pitted material on the floors of pits in both Esira and the unnamed summit pit crater indicates that central pit formation is completed prior to the solidification of impact melt. This is strong evidence that pit formation is coeval with crater formation.

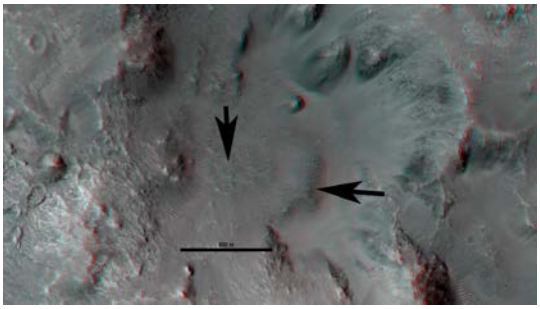

Figure 3: Pitted material (arrows) on the floor of the unnamed summit pit crater shown in Fig. 1. (HiRISE B03_010764_2161)

Comparison of Summit Pit Craters on Mars and Mercury: Our analysis of Mercury revealed the presence of 32 central pit craters, all summit pits. There was no correlation in the distribution of these summit pit craters with features associated with volatiles, including radar-bright craters at the poles or craters containing hollows [15]. We compared the ratio of the basal diameter of the central peak to the crater diameter (D_{pk}/D_c) for both pitted and unpitted central peaks on Mercury and found the ratio to be statistically identical. We conducted a similar study for summit pit craters on Mars and again found no statistical difference in the D_{pk}/D_c values for pitted and non-pitted central peaks. This indicates that summit pits form on uplifts that are indistinguishable from normal central peaks. However, D_{pk}/D_c for summit pit craters on Mars are approximately twice as large as for summit pit craters on Mercury (median value of 0.30 for Mars versus 0.15 for Mercury). This observation is additional support for the argument that Mercury's crust is stronger than the crusts of other terrestrial planets.

Conclusions and Implications for Pit Formation: The presence of central pit craters on bodies with a range of crustal volatile concentrations (from 100% to almost 0%) indicates that volatiles are not required for central pit formation. Instead, our studies are revealing that central pits form by uplift followed by collapse of weakened target material. Crustal volatiles help to weaken the target material and enhance the collapse. This results in higher numbers of central pit craters with larger median D_p/D_c values for bodies with volatile-rich crusts. However, the strength of the body's surface gravity also dictates whether central pit collapse can occur. Volatile-rich targets tend to favor formation of floor pit craters whereas summit pits become more common as the concentration of target volatiles decreases. Summit pits form on otherwise normal central peaks, where the basal diameter is determined by target strength. Our geologic mapping of fresh Martian central pit craters reveals that the high thermal inertia signature surrounding the pit is due to uplifted megablocks of bedrock with no sign of ejeted blocks produce by explosive activity, as proposed by the melt contact model [11]. The presence of pitted material on the floors of both floor and summit pits shows that pit formation occurs before the impact melt solidifies, which indicates that pits are not erosional features formed long after the crater.

Acknowledgements: This work is supported by NASA MDAP Award NNX12AJ31G and NASA PGG Award NNX14AN27G.

References: [1] Barlow N.G. (2010) *GSA SP 465*, 15-27. [2] Gillis-Davis J.J. et al. (2009) *EPSL 285*, 243-250. [3] Garner K.M.L. and Barlow N.G. (2012) *43rd LPSC*, Abstract #1256. [4] Wood C.A. et al. (1978) *Proc. 8th LPSC*, 3691-3709. [5] Croft S.K. (1981) *LPS XII*, 196-198. [6] Passey Q.R and Shoemaker E.M. (1992) *Satellites of Jupiter*, UAz Press, 379-434. [7] Greeley R. et al. (1982) *Satellites of Jupiter*, UAz Press, 340-378. [8] Senft L.E. and Stewart S.T. (2011) *Icarus 214*, 67-81. [9] Bray V.J. et al. (2012) *Icarus 217*, 115-129. [10] Elder C.M. et al. [2012] *Icarus 221*, 831-843. [11] Williams N.R. et al. (2015) *Icarus 252*, 175-185. [12] Nuhn A.M. et al. (2015) *GSA SP 518*, 65-84. [13] Tornabene L.L. et al. (2012) *Icarus 220*, 348-368. [14] Boyce J.M. et al. (2012) *Icarus 221*, 262-275. [15] Horstman R.M. and Barlow N.G. (2016) *47th LPSC*, Abstract #1156.